Supporting Information

Dragon fruit-like biocage as an iron trapping nanoplatform for high efficiency targeted cancer multimodality imaging

*Min Yang,† Quli Fan,† Ruiping Zhang,† Kai Cheng, Junjie Yan, Donghui Pan, Xiaowei Ma, Alex Lu, and Zhen Cheng**

Determination of the loading amount of MNP in AMF

The final protein concentration of AMF was determined by Bio-Rad Protein assay using bovine serum albumin as the standard. The Fe concentrations were determined by inductively coupled plasma-mass spectrometry (ICP-MS). A calibration curve of standard MNPs was established by measuring Abs_{680} of free MNP at different concentrations. The MNP content in AMF was determined by comparing Abs_{680} of AMF (subtracted protein and Fe) solution with those of a standard MNP solution.

Characterization of AMF

Absorption spectra of nanoparticles were taken using the Agilent Technologies Cary 60 UV−VIS, and exported data were graphed in origin (Fig. S1). The Dynamic Light Scattering (DLS) measurement and TEM images were taken. For the DLS measurement, water-soluble particles were directly measured in the cuvette. For TEM, sample preparation and measurement were similar to the previous report with or without uranyl staining.

Cell culture

HT29 (human colon cancer) and HepG2 (human liver cancer) cell lines were purchased from ATCC. HT29 cells were grown in McCoy's 5A medium supplemented with 10% fetal bovine serum (FBS) and 1% penicillin streptomycin (Gibco, USA). HepG2 cells

were grown in DMEM medium containing 10% FBS and 1% Pen-Strep. These two cell lines were incubated humidly under 37 °C and 5% CO_2.

Cell uptake and block experiment

HT-29 and HepG2 cells were seeded into 24-well plates at a density of 1×10^5 cells per well and incubated overnight with corresponding mediums. For cell uptake group, the cells were washed three times with PBS (pH 7.4) and then incubated with 37 kBq of ^{64}Cu labeled AMF in triplicate at 37 ^{o}C for 15, 30, 60 and 120 min. Subsequently, cells of each well were rinsed with ice-cold PBS twice and lysed with 0.1 M NaOH. The lysate were transferred to γ-counter and the radioactivity was measured. For specific blocking group, the cells were pre-incubated with apoferritin (1 μM) in serum-free medium for 1 h and then were treated just as cell uptake group. All of samples were expressed as the percentages of the added dose (%AD).

Cell binding affinity measurement

HT-29 cells were seeded into 96-well plates at a density of 1×10^5 cells per well and incubated overnight. Then the cells were washed with PBS three times. Subsequently, cells were incubated in the presence of increasing amounts of competing apoferritin (0 nM ~ 20 μM) with 37 kBq ^{64}Cu labeled AMF per well in a total volume of 200 μL at 37 ^{o}C for 60-80 min. Cells were rinsed with ice-cold PBS twice and then lysed with 0.1 M NaOH. The radioactivity of lysate was determined by γ-counter. Binding data was calculated using GraphPad Prism software.

MTT Assay

HT-29 and HepG2 cells were seeded in 96-well plates at a density of 5×10^3 cells per well for overnight incubation. The medium was removed and the medium containing a series of concentration of AMF (0 ~ 10 μM) was added in triplicate. After 12 h incubation at 37 ^{o}C, the cell cytotoxicity was quantified using a MTT Cell Proliferation and Cytotoxicity Assay Kit (Beyotime, Haimen, China). And the absorbance was chosen at 570 nm.

Animal models

All animal experiments were conducted in accordance with the Guidelines for the Care and Use of Research Animals established by the Stanford University. The tumor model was established by subcutaneous injection of cells (3×10^6 in a mixture of 100 μl of PBS) into the front flank of female athymic nude mice (BALB/C) with HT29 on the right flank and HepG2 on the left. The mice underwent imaging studies when the tumor volume reached 150-500 mm^3 (3-5 weeks after inoculation).

Data analysis

Results were expressed as the mean±standard deviation unless otherwise stated. Statistical comparisons between two groups were determined by t-test. For all tests, $P<0.05$ was considered statistically significant. All statistical calculations were performed using GraphPad Prism v.5 (GraphPad Software Inc., CA, USA).

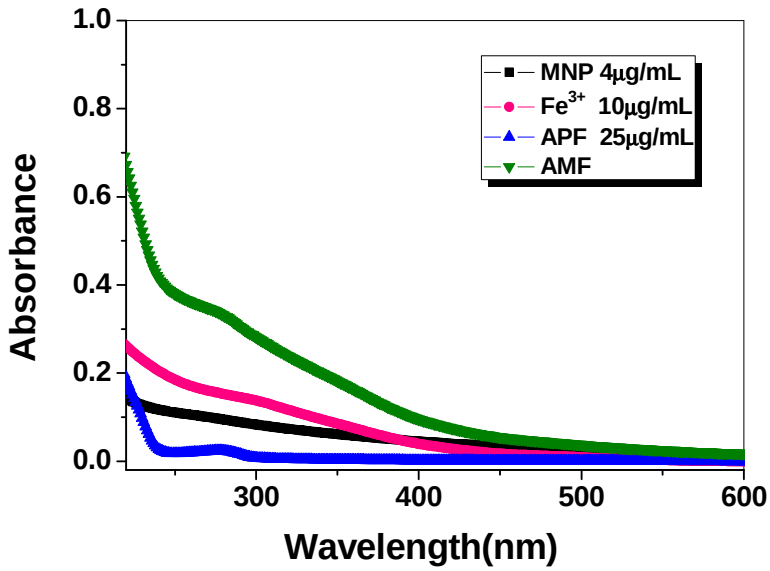

Fig. S1. UV-vis spectra of APF, MNP, $FeCl_3$ and AMF.

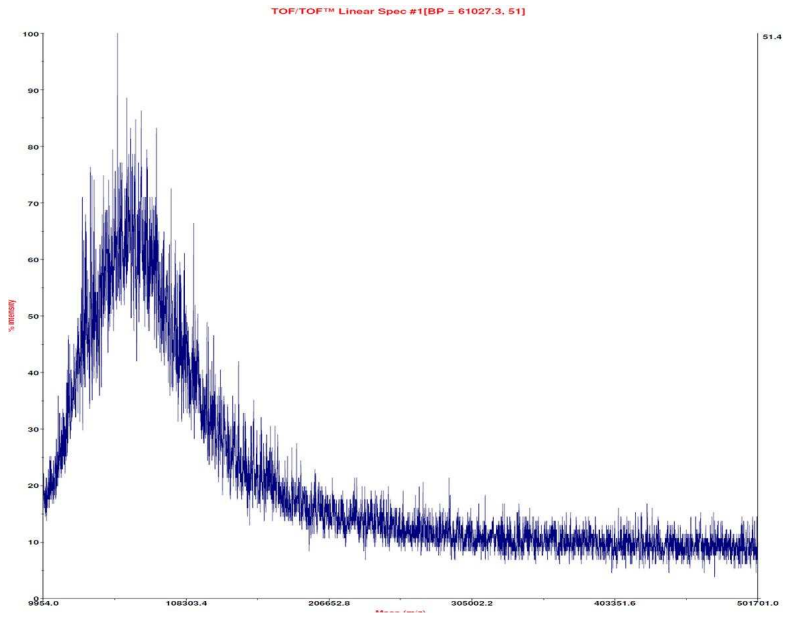

Fig. S2. MS of MNPs.

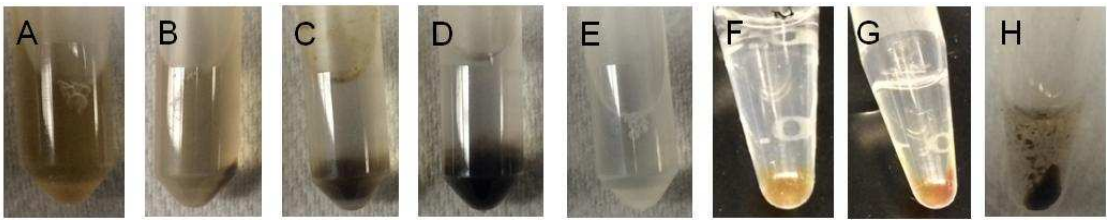

Fig. S3. Optimization conditions for Fe-MNP-APF (AMF) preparation.

A: pH~2 (open cage*), APF/MNP/Fe=1/1/1000, brown clear solution;

B: pH=7.4, APF/MNP/Fe=1/1/1000, brown precipitation;

C: pH~2 (open cage), APF/MNP/Fe=1/1/3000, black precipitation;

D: pH~2 (open cage), APF/MNP/Fe=1/3/3000, black precipitation;

E: pH=7.4, APF/Fe=1/1000 in 1 mL, pale yellow precipitation;

A-E: Total volume is 1 mL;

F: pH~2 (open cage), APF/Fe=1/1000 in 0.2 mL, clear, then pass NAP-5, collect 0.5 mL, red brown precipitation;

G: pH~2 (open cage), APF/Fe=1/2000 in 0.2 mL, clear, then pass NAP-5, collect 0.5 mL, red brown precipitation;

H: conditions like open cage, MNP/Fe=1/1000 in 0.2 mL, black precipitation.

*Open cage: APF is protein with cage-like structure, it disassembles into subunits at acid conditions, and we describe the encapsulation of Fe^{3+} and MNP under this circumstance as “open cage”.

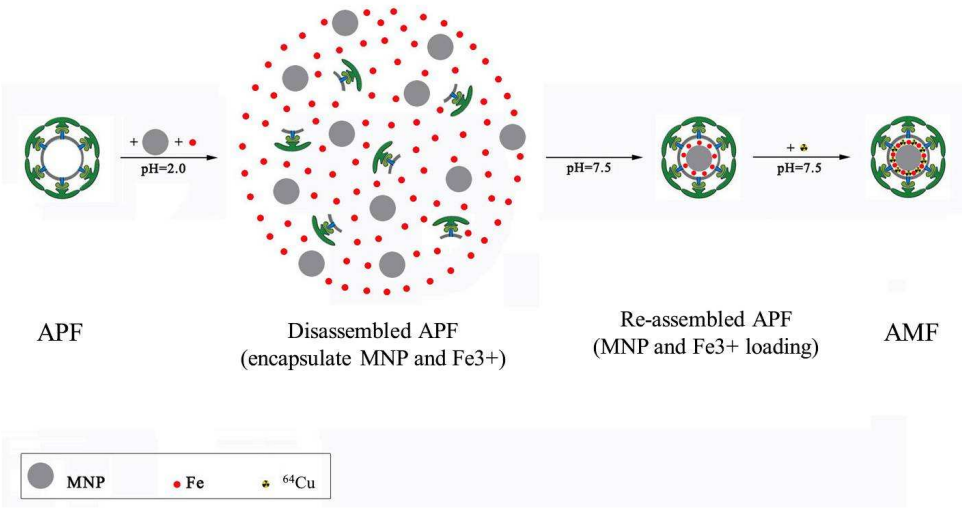

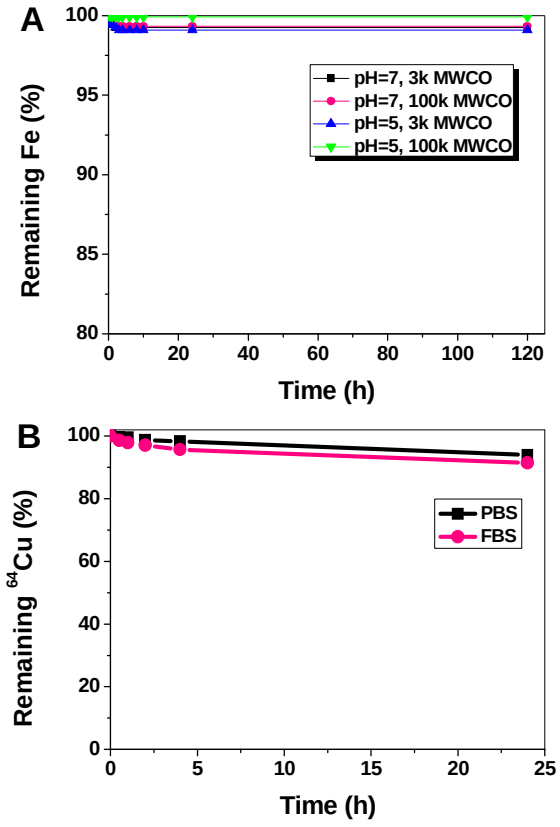

Fig. S4. Stability of Fe^{3+} in AMF (A) and $^{64}Cu^{2+}$ in ^{64}Cu-AMF (B).

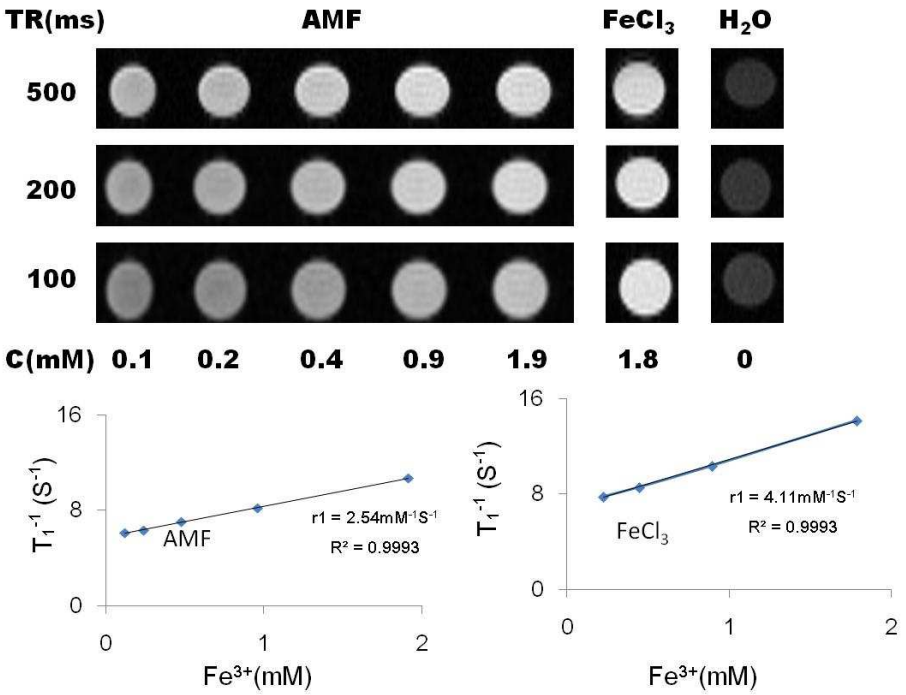

Fig. S5. T_1 MR images (up) and T_1 relaxation rate ($1/T_1$) as a function of Fe^{3+} concentrations for AMF (left, down) and $FeCl_3$ phantoms (right, down).

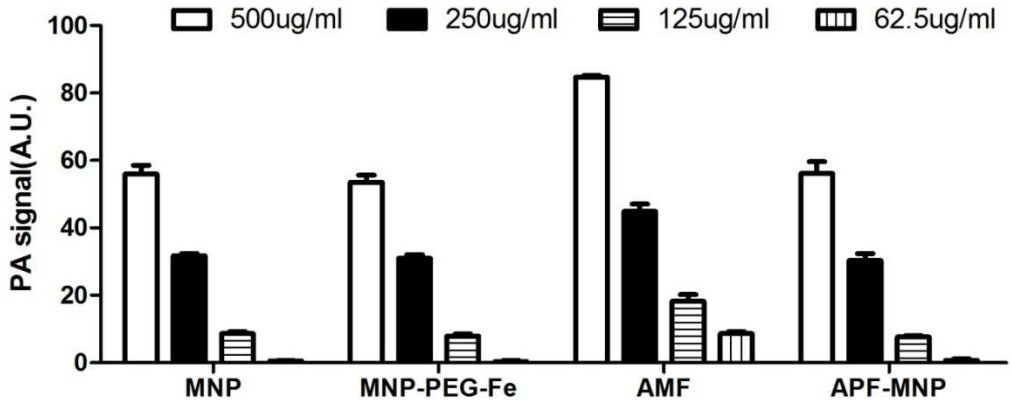

Fig. S6. PA signals of MNP, MNP-PEG-Fe, AMF, APF-MNP (AMF without Fe) phantoms (Concentration based on MNP amount). AMF shows significant higher PA signal intensities than those of MNP, MNP-PEG-Fe, and APF-MNP at all concentrations ($p<0.01$), whereas the PA signal intensity of MNP shows no statistical difference from MNP-PEG-Fe and APF-MNP ($p>0.05$).

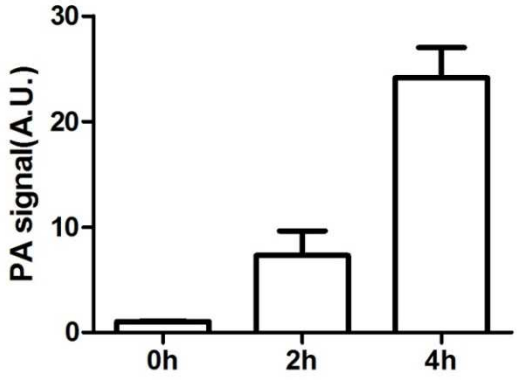

Fig. S7. PAI signal of AMF in HT29 tumor-bearing mice.

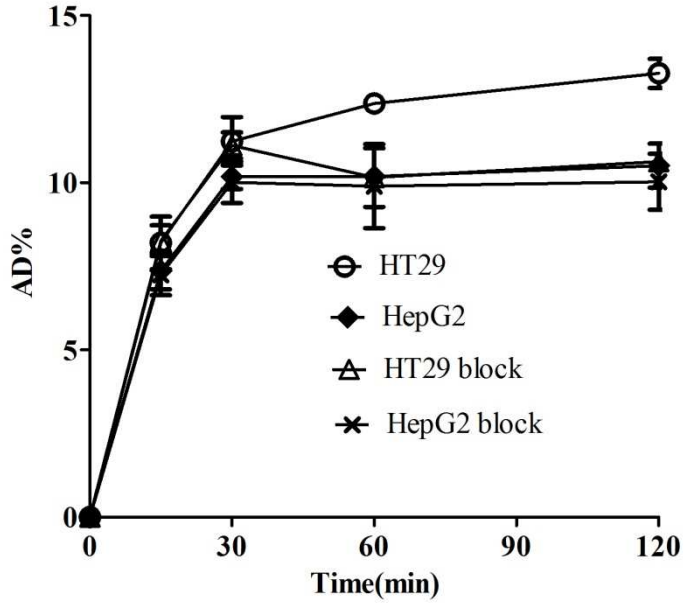

Fig. S8. Uptake of ^{64}Cu labeled AMF with and without blocking dose of AMF in HT29 and HepG2 cells.

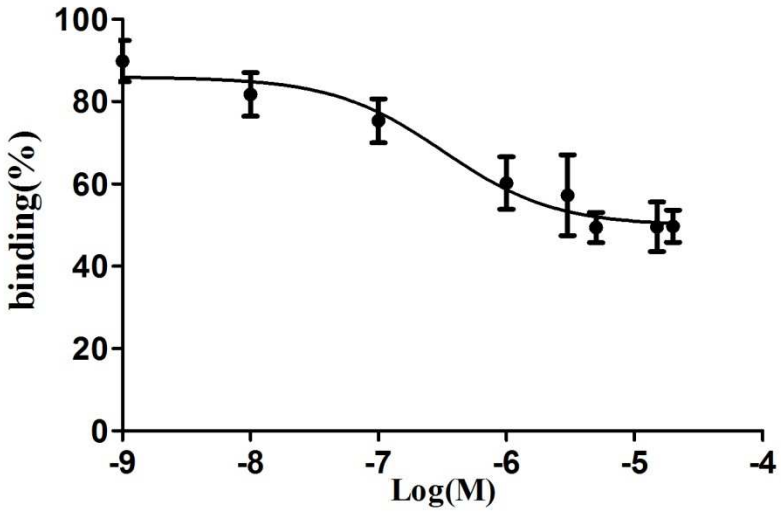

Fig. S9. Binding competetion of ^{64}Cu labeled AMF to HT-29 cells with a series of concentration of APF.

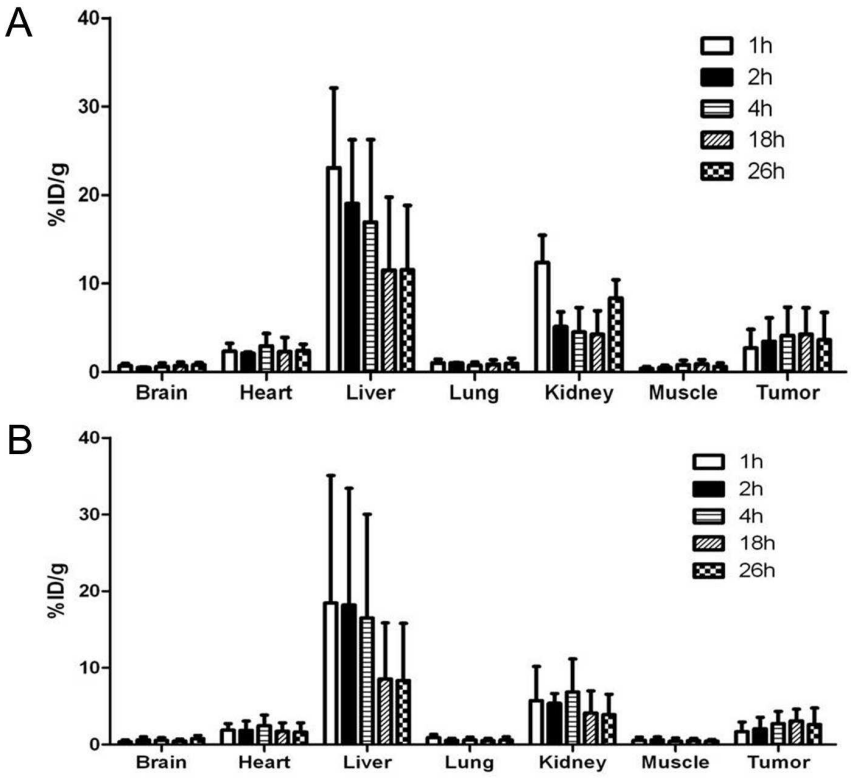

Fig. S10. Biodistribution of ^{64}Cu labeled AMF in HT29 (A) and HepG2 (B) tumor bearing mice (n = 4) at 1, 2, 4, 18 and 26 h after injection.

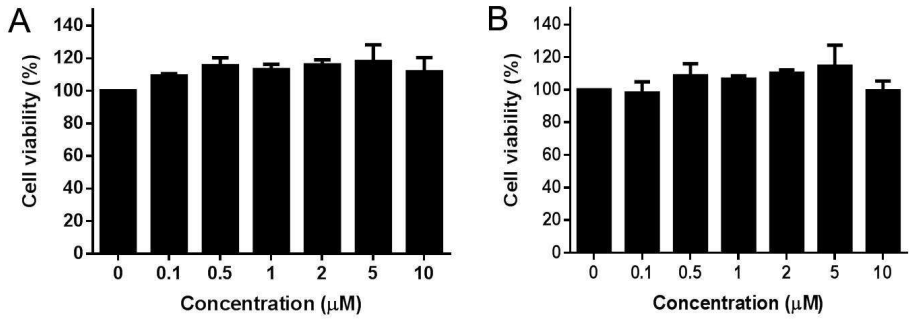

Fig. S11. MTT assay using HT29 (A) and HepG2 (B) cells with AMF concentration 0.1, 0.5, 1, 2, 5 and 10 μM.

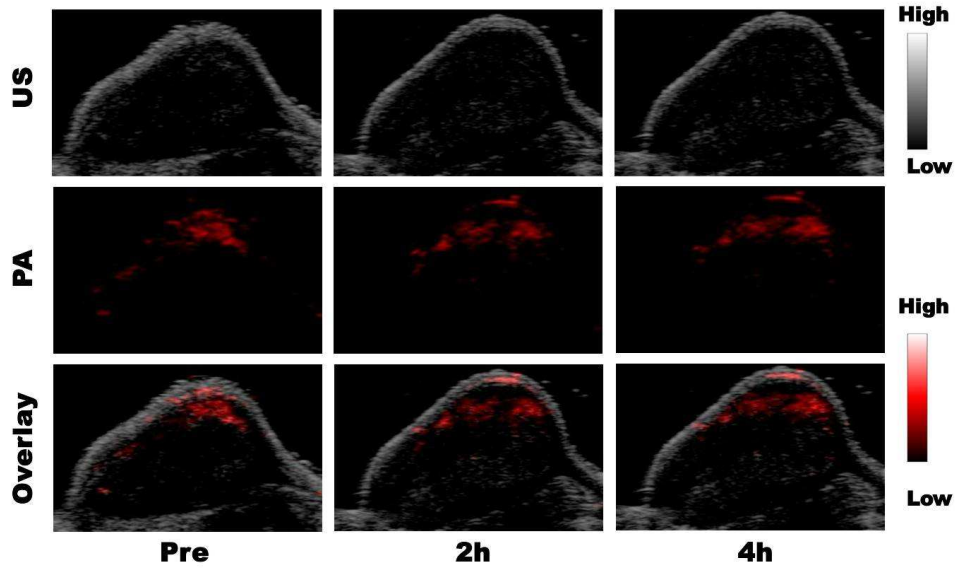

Fig. S12. The US (grey, top), PA (red, middle) and overlayed coronal sections (bottom) of HepG2 tumor models before and after tail-vein injection of AMF nanocages.

Table S1. The data of hydrodynamic sizes and zeta potentials of APF, MNP and AMF in aqueous solution.

Sample	Diameters(nm)	Zeta Potential
APF	13.6±1.4	-17.2±4.5
MNP	5.6±0.4	-31.8±3.0
AMF	16.4±0.3	-18.4±6.1